Article

Not peer-reviewed version

Effortless One-Pot Two-Step Creation of NiS-NiO/S-g-C3N4: The Next Generation Photocatalyst for Green C(sp3)-F Bond Activation and Coenzyme Regeneration

Sanjana Kumari , Rajesh K. Yadav * , Satyam Singh , Rehana Shahin , Suresh Kumar Pandey , Kamini Singh , Atul Partap Singh , Navneet Kumar Gupta , Dhanesh Tiwary , D. K. Dwivedi *

Posted Date: 13 July 2023

doi: 10.20944/preprints202307.0866.v1

Keywords: NiS-NiO/S-g-C3N4 photocatalyst 1; C(sp3)-F Bond Activation 2; Regeneration of Coenzyme 3; Solar Light 4; Selectfluor 5 doi:10.20944/preprints202307.0866.v1

Article

Effortless One-Pot Two-Step Creation of NiS-NiO/S-g-C_3N_4: The Next Generation Photocatalyst for Green C(sp3)-F Bond Activation and Coenzyme Regeneration

Sanjana Kumari [1], Rajesh K. Yadav [1]*, Satyam Singh [1], Rehana Shahin [1], Suresh Kumar Pandey [2], Kamini Singh [3], Atul P. Singh [4], Navneet Kumar Gupta [4], Dhanesh Tiwary [2] and Dilip K. Dwivedi [5]*

[1] Department of Chemistry and Environmental Science, Madan Mohan Malaviya University of Technology, Gorakhpur-273010, U. P., India
[2] Department of Chemistry, Indian Institute of Technology (BHU), Varanasi 221005, India
[3] Department of Chemistry, Deen Dayal Upadhyaya University Gorakhpur, Gorakhpur-273009, U.P. India
[4] Department of Chemistry, Chandigarh University, Mohali,140413, Punjab, India.
[5] Centre for Sustainable Technologies, Indian Institute of Science, Gulmohar Marg, Mathikere, Bengaluru 560012, India
[5] Department of Physics and Materials Science, Madan Mohan Malaviya University of Technology, Gorakhpur 273010, India
* Correspondence: rajeshkr_yadav2003@yahoo.co.in (R.K.Y.); todkdwivedi@gmail.com (D.K.D.)

Abstract: Fluorinated compounds and co-enzymes are being widely researched and employed throughout research community because of their versatile physical, chemical and biological properties. In this work, we synthesized NiS-NiO/S-g-C_3N_4, a highly effective photocatalyst for C(sp^3)-F bond activation and the regeneration of coenzyme (1,4-NADH) employing a new and ecologically acceptable route. The obtained photocatalyst exhibited important photocatalytic properties, such as good solar light harvesting ability, suitability of the optical band-gap, and facilitating efficient charge migrations. As a result, the newly designed NiS-NiO/S-g-C_3N_4 photocatalyst shows the excellent yield for regenerations of 1,4-NADH (51%). Further, a method of combining C(sp^3)-F bond activation with photocatalysis has been demonstrated that represents a very powerful and sustainable approach, that can be a major breakthrough for the field of pharmaceutical.

Keywords: NiS-NiO/S-g-C_3N_4 photocatalyst 1; C(sp^3)-F bond activation 2; regeneration of coenzyme 3; solar light 4; selectfluor 5

1. Introduction

The ever-increasing environmental concerns has led researchers worldwide to develop visible light responsive photocatalyst which is highly active and inexpensive for effective environmental remediation [1–4]. Among the several experimental methods, photocatalysis is being employed mostly for the solar-driven organic transformations because of abundant availability of solar energy which is renewable energy resource [5–7]. The formations of solar chemicals based on green technology has emerged as asignificant research area. In the numerous enzymes based photocatalytic reactions, the reduced forms of nicotinamide adenine dinucleotide (NADH) act as a proton donor along with electron. Although, NADH is an essential component for many enzymatic reactions still using the conventional method for the regeneration of NADH possess some limitations such as, poor-selectivity, costly, excessive toxicity and poor long-term stability [8–12]. Hence for the regeneration of NADH, the synthesis of effective photocatalyst is of utmost importance. Moreover, with the growing requirement of fluorinated compounds which are used as pharmaceuticals and agrochemicals there is upsurge in research and development of new approaches to perform selective fluorination [13,14]. Amongst various enabling technologies, artificial photocatalysis is an effective approach for the regeneration coenzyme of NADH and fluorinated compounds because of the use of sustainable and environment-friendly solar light [15-17]. To facilitate artificial photosynthetic process two-dimensional layered materials of graphitic carbon nitride (g-C_3N_4) has gained wide consideration due to its versatile property such as excellent optical characteristics and excellent thermal stability [18-20]. Although pristine g-C_3N_4 has been utilized in the photocatalytic applications, but wide optical band gap limits its advantageous properties [19]. Doping of heteroatom such as sulfur in g-C_3N_4 is one of the methods to tune the optical band gap forming so-called sulfur doped graphitic carbon nitride(S-g-C_3N_4). From previous studies, it has been reported that doping of sulfur into the g-C_3N_4 results in better charge separation as it brings about the separation among lowest unoccupied molecular orbitals (LUMOs) and highly occupied molecular orbitals (HOMOs) [21-23]. We believe that hybridizing NiS-NiO with S-g-C_3N_4 could again improve the action of the resultant photocatalyst under solar light. Therefore, in this study NiS-NiO/S-g-C_3N_4 photocatalyst was synthesized and used for efficient activation of C(sp^3)-F bond and regeneration of 1,4-NADH. In this article, we reported an environmentally friendly, scalable, inexpensive and simple method for the synthesized of heterostructured NiS-NiO/S-g-C_3N_4 photocatalyst for regeneration of 1,4-NADH and activation of C(sp^3)-F bond. The successful formation mechanism of NiS-NiO/S-g-C_3N_4 photocatalyst is elucidated conferring to a series of structural characterizations and experiments. It is shown that the heterostructure composed of NiS-NiO and S-g-C_3N_4 exhibited improved catalytic activity. Further, a method of combining fluorination with photocatalysis (photo fluorination) has been demonstrated that signifies a very influential and greener approach has reported in literature [24,25].

2. Materials and Methods

2.1. Experimental Section

The following chemicals, Thiourea (T), Dimethylformamide (DMF), Nickel acetate (Ni $(CH_3COO)_2$, elemental sulfur, buffer solution, Nicotinamide adenine dinucleotide (NAD^+), Ascorbic acid (AsA), Selectofluor(F-TEDA), Acetonitrile (ACN), Potassium carbonate (K_2CO_3), 4-formylbenzoic acid, Acetone (CH_3COCH_3), sodium sulphate (Na_2SO_4), were purchased from Sigma-Aldrich and used as obtained.

2.2. Design of an Artificial Photosynthetic System

In this study we utilized NiS-NiO/S-g-C_3N_4photocatalyst for the production of NADH from NAD^+ by consuming solar rays. (Scheme 1). shows the NAD^+ to NADH production in artificial photocatalytic system under solar light. The visible light absorption causes excitation of electron by NiS-NiO/S-g-C_3N_4 photocatalyst and transferred to rhodium complex $[Cp^*Rh(bpy)H_2O]^{2+}$. Further the reduction of NAD^+ to NADH take place as electrons are transferred from rhodium complex to NAD^+. Hence between NiS-NiO/S-g-C_3N_4 photocatalyst and NAD^+, rhodium complex act as a efficient mediator of electron[26,27].

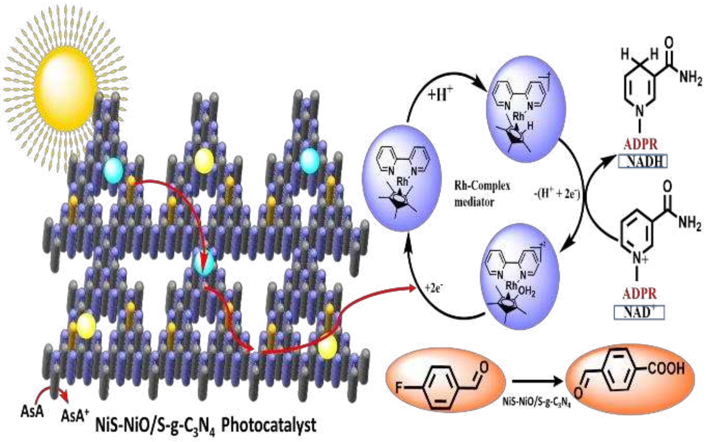

Scheme 1. Illustration of the mechanism of artificial photosynthetic pathway for 1,4-NADH regeneration and C(sp^3)-F bond formation.

2.3. Synthesis of S-g-C$_3$N$_4$

The sulfur doped-g-C$_3$N$_4$ (S-g-C$_3$N$_4$) material was synthesized via the thermal condensation method as shown in Scheme 2. Initially 10g thiourea (T) was taken in crucible and treated at 300°C temperature for 2 h in muffle furnace under inert air (Scheme 2). As a result, yellow colour powder was obtained which was further dissolved in DMF and stirred for 24 hours and was deconned. For one week the same procedure of dissolving in DMF, stirring and deconning was repeated. Thereafter the product obtained after deconning was mixed with buffer solution by stirring for 30 min. Finally with continuous heating at 153°C for 1 hour the solvent was evaporated that resulted in formation of yellow precipitate. After filtration the compound obtained on filter paper was kept overnight at 70°C in oven for drying. The obtained soft powder was of S-g-C$_3$N$_4$ [28,29].

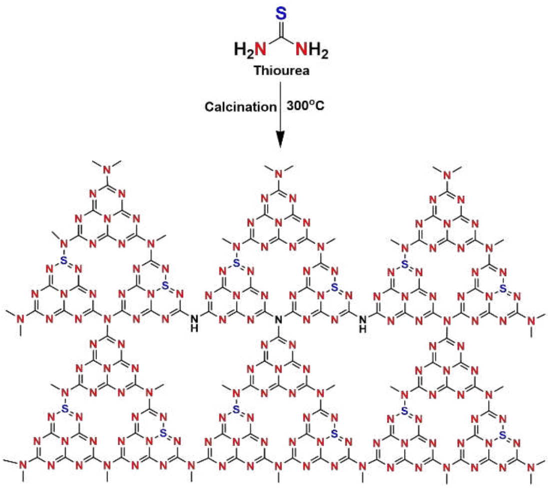

Scheme 2. Synthesis of S-g-C$_3$N$_4$powder.

2.4. Synthesis of NiS-NiO/S-g-C$_3$N$_4$ photocatalyst

To synthesis the NiS-NiO/S-g-C$_3$N$_4$photocatalyst, 500 mg S-g-C$_3$N$_4$ powder, 150mg nickel acetate as source of nickel, and 150mg elemental sulfur were crushed using ball milling method till the formation of green-yellowish fine mixture powder. After the formation of mixture powder, we placed the mixture in muffle furnace for 2 hrs. at 400°C for calcination process. Finally, we get heterostructured NiS-NiO/S-g-C$_3$N$_4$ photocatalyst in the form of powder, In the last step we wash the heterostructured NiS-NiO/S-g-C$_3$N$_4$ photocatalyst with distilled water (Scheme 3) [26,27].

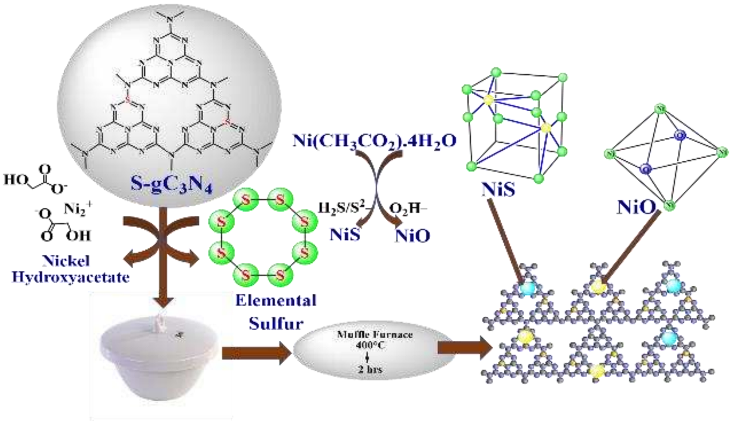

Scheme 3. Synthesis of NiS-NiO/S-g-C$_3$N$_4$ composite photocatalyst.

3. Results

The optical band gap in NiS-NiO/S-g-C_3N_4 photocatalyst system was investigated using diffuse reflectance spectroscopy (DRS). The optical property of NiS-NiO/S-g-C_3N_4 photocatalyst was studied by UV visible absorption spectra as shown in (Figure 1) and compared with S-g-C_3N_4 by literature [28]. The broad peak at 538 nm was obtained for NiS-NiO/S-g-C_3N_4 photocatalyst. Whereas a peak at 455 nm was obtained for S-g-$C_3N_4$by previous study [28]. Using Scherrer equation the optical band gap of S-g-C_3N_4 and NiS-NiO/S-g-C_3N_4 photocatalysts were calculated to be 2.72eV and 2.30 eV, respectively. The optical band gap value of NiS-NiO/S-g-C_3N_4 photocatalysts was also confirmed using Tauc plot (shown in inset Figure 1). The decrease optical band gap of the NiS-NiO/S-g-C_3N_4 photocatalysts performs excellent result in the visible light for C(sp^3)-F Bond Activation and Regeneration of Coenzyme [29,30].

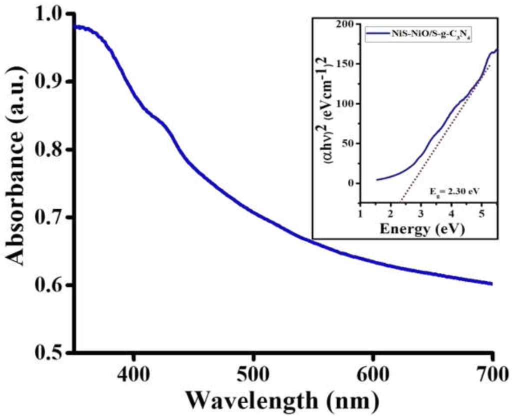

Figure 1. UV-Visible Spectroscopy and Tauc Plot of NiS-NiO/S-g-C_3N_4 photocatalyst.

The FTIR spectra of S-g-C_3N_4 and NiS-NiO/S-g-C_3N_4 photocatalysts are shown in (Figure 2), confirming the presence of NiS and NiO in the nanocomposite. The vibrational spectrums of S-g-C_3N_4 in which the stretching vibration of the C-N bond is assigned to the representative characteristic peaks at 2065, 1045, 920, 870, and 775 cm^{-1} [28,31]. The broad absorption peaks in the range 3600-2555 cm^{-1} shows its non-crystalline nature and associated to N-H stretching vibration modes. Furthermore, multiple peaks from 1635-1325 cm^{-1} can be accredited to C-N and C=N stretching mode of the aromatic unit, whereas some peaks at 775 cm^{-1} verified with triazine unit. Further, the broad peak at 1100 cm^{-1} appears, which confirm the stretching vibration of the C-S bond, confirming the doping of sulfur (S) within the graphitic carbon nitride (C–N) lattice. For vibrational spectrums of NiS-NiO/S-g-C_3N_4, all the transmittance peaks reduced and shows blue shifting which confirms the loading of NiS and NiO nanoparticles on S-g-C_3N_4. Herein, the characteristic peaks are found at 2154, 1100, 885, 805, 679 cm^{-1}. The sulphide has an absorption band at 1100 cm^{-1}. The presence of Ni-S bond is indicated by absorption band at 679 cm^{-1} [32-34].

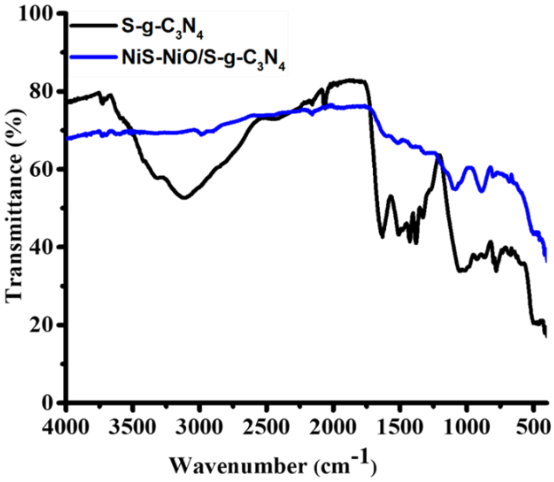

Figure 2. Fourier-Transform Infrared (FT-IR) spectra of S-g-C_3N_4 powder and NiS-NiO/S-g-C_3N_4 photocatalyst.

The average particle size (d) and zeta potential (ξ) of S-g-C_3N_4 and NiS-NiO/S-g-C_3N_4 photocatalysts were investigated using the dynamic light scattering (DLS) approach. The particle size (Figure 3) of NiS-NiO/S-g-C_3N_4 photocatalysts was approx. five time smaller than S-g-C_3N_4, it's clearly showed that there was successfully formation of NiS-NiO/S-g-C_3N_4 photocatalyst from S-g-C_3N_4. In other words, NiS-NiO/S-g-C_3N_4 photocatalyst is more efficient than S-g-C_3N_4 due to the smaller particle size and fast charge transfer rate of NiS-NiO/S-g-C_3N_4 photocatalyst. The formation of NiS-NiO/S-g-C_3N_4 photocatalyst is also supported by zeta potential studies. Zeta potential (ξ) (Figure 4) of S-g-C_3N_4 (-35.60 mV) is less negative than zeta-potential of NiS-NiO/S-g-C_3N_4 photocatalyst (-5.30 mV) which clearly indicated the successful formation of NiS-NiO/S-g-C3N4 photocatalyst from S-g-C_3N_4 [35,36].

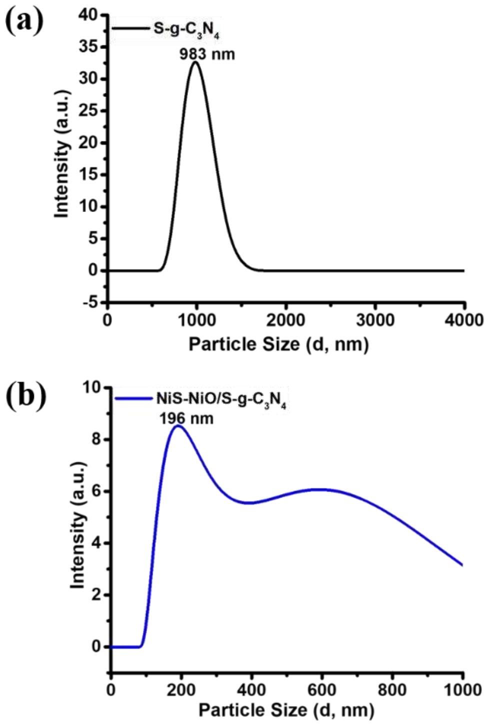

Figure 3. Particle size of (a) S-g-C_3N_4 powder and (b) NiS-NiO/S-g-C_3N_4 photocatalyst.

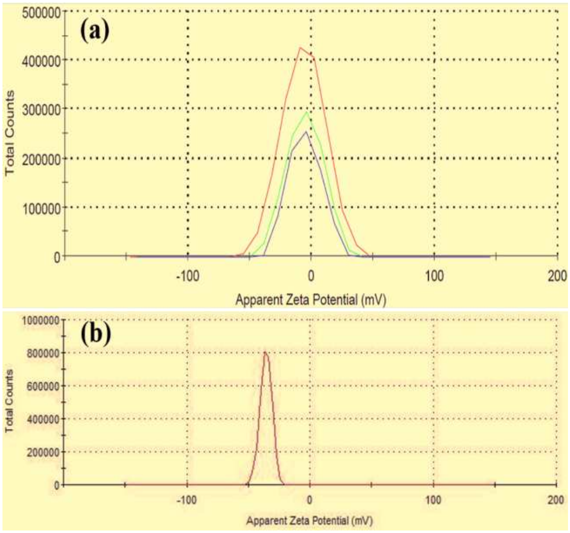

Figure 4. Zeta potential of (a) S-g-C_3N_4 powder and (b) NiS-NiO/S-g-C_3N_4 photocatalyst.

Figure 5(a) and 5(b) shows the cyclic voltammetry and Latimer diagram of NiS-NiO/S-g-C_3N_4 photocatalyst that estimated the electrochemical properties of the photocatalyst. From CV study, E_{red}, E_{oxd}, and electronic band gap of NiS-NiO/S-g-C_3N_4 photocatalyst were obtained as -0.91 V, 1.36V, and 2.27 V, respectively. This value is also satisfied by Tauc plot and represented through Latimer diagram. Therefore, the HOMO and LUMO energy levels of NiS-NiO/S-g-C_3N_4 photocatalyst were obtained as -5.86 eV and -3.59 eV respectively. Under solar light, electron transfer from the increased HOMO value of the photocatalyst allows for selective radical–radical coupling. It indicates the suitable energy band gap for NADH regeneration and C(sp^3)-F bond activation [37,38].

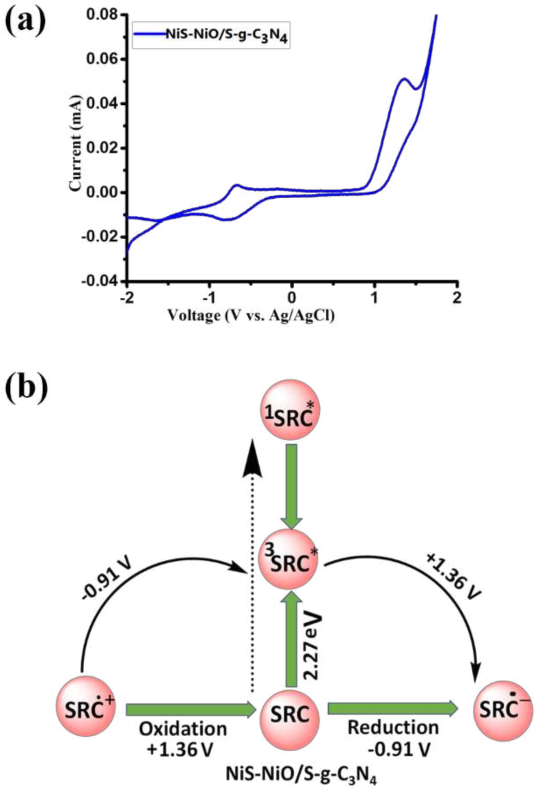

Figure 5. (a) Cyclic Voltametric and (b) Latimer diagram of NiS-NiO/S-g-C_3N_4 photocatalysts.

4. Applications of NiS-NiO/S-g-C_3N_4 photocatalyst

*4.1. A Plausible mechanism for the 1,4-NADH co-factor regeneration through a [Cp*Rh(bpy)Cl] Cl*

Mechanism studies for the solar light induced NADH regeneration using NiS-NiO/S-g-C_3N_4 photocatalyst is depicted in Scheme 4. During solar light induced catalytic reaction, the cationic state of Rh complex formed undergo hydrolysis, which give the water coordinated complex (A). The formate ($HCOO^-$) react with the complex (A) via hydride elimination process to produce complex (B) with removal of CO_2molecule. The reduced form of complex (D)is formed after the suppling of charges to the complex C by the NiS-NiO/S-g-C_3N_4 photocatalyst. Finally, NAD^+ is reacts with the reduced complex (D) through its amide group and hydride ion transfer also takes place simultaneously (complex E and F) to regenerates selective NADH co-factor [39,40].

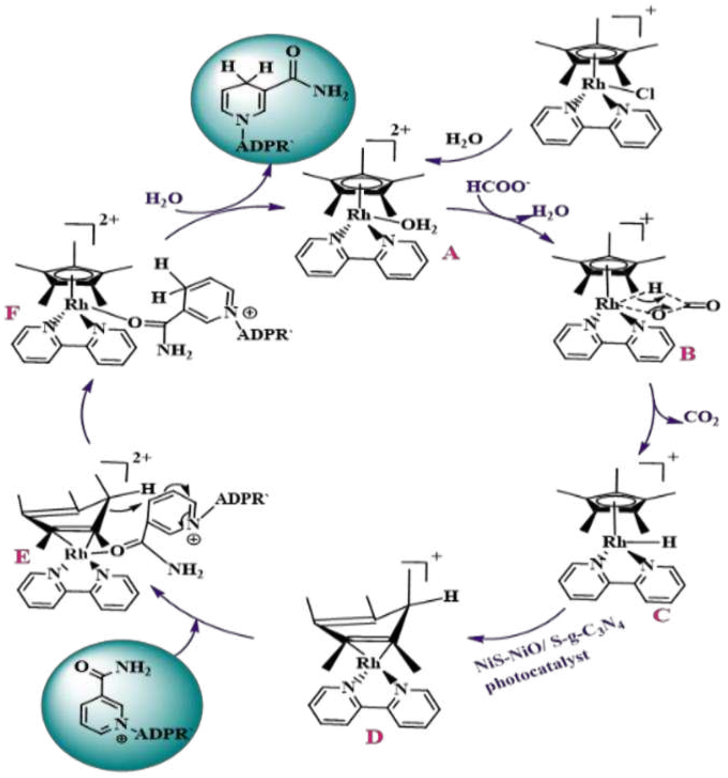

Scheme 4. The mechanistic pathways through for regioselective 1,4-NADH cofactor regeneration.

4.2. *The route of carrier formation and migration in an artificial photocatalytic system*

The charge carrier generation and transfer during artificial photocatalysis is depicted in (Scheme 6). Initially, solar light irradiation results the formation of photoexcited electron-hole in the valence band of NiS-NiO/S-g-C_3N_4 [energy, −5.86 eV]. The electron-hole is quenched by ascorbic acid (AsA) [energy, -5.25 eV] and transporting the photoexcited electrons into the conduction band [energy− 3.59 eV] of NiS-NiO/S-g-C_3N_4 and then to NAD^+ [energy, − 4.20 eV] via rhodium complex mediator [energy, -3.96 eV] and take part in regioselective 1,4-NADH regeneration [41-44].

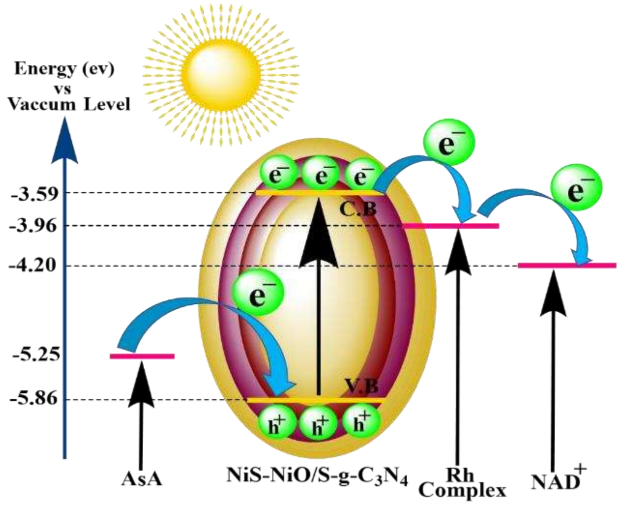

Figure 6. The energy diagram demonstrating carrier formation and their migration in the artificial photocatalytic system.

4.3. *Photocatalytic Regenerations of NADH*

Using 450 W halogen lamp with a cutoff filter of 420 nm as source of light the photocatalytic NADH cofactor regeneration was performed. The procedure was performed at room temperature under inert atmosphere. The photocatalytic reaction medium consists AsA (310 μL), β–NAD^+ (248 μL), electron mediator (124 μL), and NiS-NiO/S-g-C_3N_4 photocatalyst (31 μL) in 3.1 mL of sodium phosphate buffer 2387 μL (pH 7.0).The absorption peak at 340 nm shows the accumulation of NADH in the existence of NiS-NiO/S-g-C_3N_4 photocatalyst. From the literature data, the molar absorption coefficient of NADH is found to be e = 6300 mol^{-1} cm^{-1} (at 340 nm). As shown in Figure 7, When the experiment is performed in the dark it showed no reduction of oxidized form of $NAD^{+.}$ The regeneration yield of 51% of NiS-NiO/S-g-C_3N_4 photocatalyst was obtained in 2 hr. The photogeneration yield of S-g-C_3N_4 under the same conditions was obtained as 25%. This demonstrates that the NiS-NiO/S-g-C_3N_4 photocatalyst is more efficient for the regeneration of NADH than S-g-C_3N_4 [30,44-46].

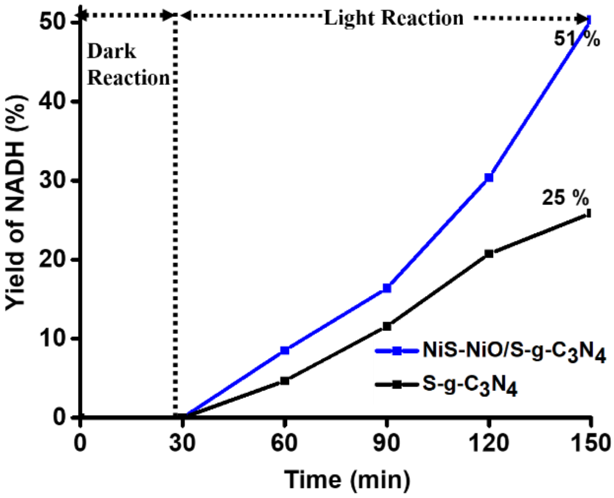

Figure 7. Photocatalytic activity of S-g-C_3N_4 powder and NiS-NiO/S-g-C_3N_4 photocatalyst for NADH regeneration under solar light.

4.4. Photocatalytic Generation of C(sp^3)-F Bond

C(sp^3)-F bond activation of 4-formylbenzoic acid with selectofluor has been carried out at room temperature under solar light. We have developed a photocatalyst NiS-NiO/S-g-C_3N_4 to perform its photocatalytic action. For C(sp^3)-F bond activation, the reaction medium was prepared by mixing 0.4 mM Selectofluor, 0.23 mM K_2CO_3, 0.05 mM 4-formylbenzoic acid, 0.125 mM NiS-NiO/S-g-C_3N_4, 5 ml acetonitrile in 15 ml voil. The reaction was performed at room temperature under solar light. After workup, the crude product was obtained [16,17].

4.5. Activation of C(sp^3)-F Bond via NiS-NiO/S-g-C_3N_4 Photocatalyst: Its mechanism

Hammond firstly proposed a mechanism for the activation of C(sp^3)-F bond in presence of expensive metal photocatalyst as per reported literature [24,25]. Traditionally, the creation of holes and electron was done by the photoexcitation of NiS-NiO/S-g-C_3N_4 photocatalyst. In the mechanistic route firstly, 4-formylbenzoic acid was oxidized by created holes (h^+) and generating a radical undergoes very fast decarboxylation for creating the corresponding phenyl radical. Consequently, the desired fluorinated product was delivered by the phenyl radical interacting with selectofluor, and create $TEDA^{2+*}$ and acts as a radical chain carrier. Additionally, The NiS-NiO/S-g-C_3N_4 photocatalyst can access $TEDA^{2+*}$ through single electron transfer (SET) of select fluor for the resulting fluorinated product (shown in Scheme 5) [16,17,46-50].

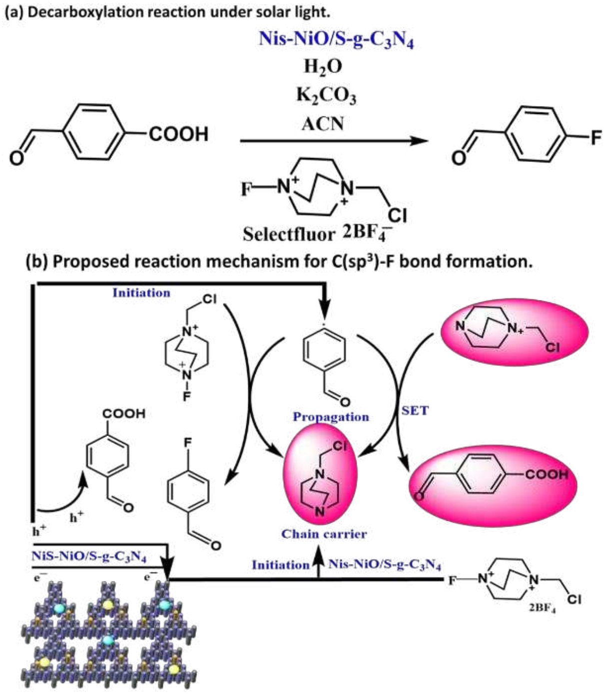

Scheme 5. Decarboxylative fluorination via NiS-NiO/S-g-C_3N_4 photocatalyst under solar light.

5. Conclusions

We have synthesized facile one-pot two-step synthesized S-g-C_3N_4 and NiS-NiO/S-g-C_3N_4 photocatalysts for C(sp^3)-F bond activation and coenzyme regeneration. The synthesized NiS-NiO/S-g-C_3N_4 photocatalyst was analyzed by UV-vis spectroscopy, FT-IR, zeta potential analysis, cyclic voltammetry and particle size analysis. Due to the high stability and excellent light harvesting property of the NiS-NiO/S-g-C_3N_4 photocatalyst, displayed the outstanding activity during the C(sp^3)-F bond activation reaction. The regeneration yield of 1,4-NADH coenzyme was achieved two-fold (51%) by using NiS-NiO/S-g-C_3N_4 photocatalyst than S-g-C_3N_4in 2 hr. The heterostructured synthesis of NiS-NiO/S-g-C_3N_4 photocatalyst shows a benchmark example in multifarious photocatalytic application.

Acknowledgements: We are very thankful to Department of Chemistry and Environmental Science of Madan Mohan Malaviya University of Technology, Gorkhpur-273010.

References

1. M. S. Dresselhaus,I. L. Thomas, Alternative energy technologies. Nature,414, (2001), 332–337, https://doi.org/10.1038/35104599.
2. L. Zhang,Y. Zhu, A review of controllable synthesis and enhancement of performances of bismuth tungstate visible-lightdriven photocatalysts. Catal. Sci. Technol., 2, (2012),694–706, 10.1039/c2cy00411a.
3. T. Le Lee, V.-D. Lim, D.; Y.-C. Lin, G. M Morris,A. L. Wong, A. J Olson,J. H. Elder, C.-H. Wong, Development of a New Type of Protease Inhibitors, Efficacious against FIV and HIV Variants. J. Am. Chem. Soc.,121, (1999), 1145–1155, https://doi.org/10.1021/ja982893p
4. C.-Y. Su, H. Li, Cheng, Z.-Q W. Liu,Li, Hou, Z. F.- Q. Bai, H.-X. Zhang, T.-Y. Ma, ZincAir Batteries: Atomic Modulation of FeCo−Nitrogen−Carbon Bifunctional Oxygen Electrodes for Rechargeable and Flexible All-Solid-State Zinc−Air Battery. Adv. Energy Mater., 7,(2017) , 13, https://doi.org/10.1002/aenm.201770067
5. D. Ravelli, S. Protti, M. Fagnoni, Application of Visible and Solar Light in Organic Synthesis. Applied Photochemistry, (2016), 281–342, 10.1007/978-3-319-31671-0_6
6. S. Protti, M. Fagnoni, The sunny side of chemistry: green synthesis by solar light. Photochemical & Photobiological Sciences, 11, (2009), 1499, https://doi.org/10.1039/B909128A

7. A. Gupta, J. R. Saurav, S. Bhattacharya, Solar light-based degradation of organic pollutants using ZnOnanobrushes for water filtration, RSC Advances, 87, (2015), 71472–71481, https://doi.org/10.1039/C5RA10456D
8. J. Kim, S. H. Lee, F. Tieves, D. S. Choi, F.Hollmann, C. Paul, C. B. Park,. Biocatalytic C=C Bond Reduction through Carbon Nanodot-Sensitized Regeneration of NADH Analogues.Angew. Chem. Int. Ed. (2018) https://doi.org/10.1002/anie.201804409
9. S. H. Lee, D. H. Nam, J. H. Kim, J.-O.Baeg, C. B. Park, Eosin Y-Sensitized Artificial Photosynthesis by Highly Efficient Visible-Light-Driven Regeneration of Nicotinamide Cofactor. ChemBioChem, 10, (2009), 1621–1624, 10.1002/cbic.200900156
10. S. H. Lee, J. H. Kim, C. B. Park, Coupling Photocatalysis and Redox Biocatalysis Toward Biocatalyzed Artificial Photosynthesis. Chemistry - A European Journal, 19, (2013), 4392–4406, https://doi.org/10.1002/chem.201204385.
11. D. H. Nam, S. H. Lee, C. B. Park, CdTe, CdSe, and CdS Nanocrystals for Highly Efficient Regeneration of Nicotinamide Cofactor Under Visible Light. Small, 6,(2010), 922–926, https://doi.org/10.1002/smll.201000077.
12. D. H. Nam, C. B. Park, Visible Light-Driven NADH Regeneration Sensitized by Proflavine for Biocatalysis. ChemBioChem, 13, (2012), 1278–1282, https://doi.org/10.1002/cbic.201200115.
13. M. Rueda-Becerril, O.Mahé, M. Drouin, M. B. Majewski, J. G. West, M. O. Wolf, … J.-F. Paquin, Direct C–F Bond Formation Using Photoredox Catalysis. Journal of the American Chemical Society, 136, (2014), 2637–2641, https://doi.org/10.1021/ja412083f.
14. T. Koike, M. Akita, Photoredox Catalysis in Fluorination and Trifluoromethylation Reactions. Organofluorine Chemistry, (2021), 225–240, https://doi.org/10.1002/9783527825158.ch7
15. M. O. Zubkov, M. Kosobokov, V. V. Levin, V. Kokorekin, A. Korlyukov, J. Hu, A. Dilman, Novel photoredox-active group for the generation of fluorinated radicals from difluorostyrenes. Chemical Science. Chem. Sci., ,11, (2020), 737-741, DOIhttps://doi.org/10.1039/C9SC04643G
16. G. Tarantino, C. Hammond, Catalytic formation of C(sp3)-F bonds via heterogeneous photocatalysis. ACS Catalysis. ACS Catal. 8, (2018), 10321–10330, https://doi.org/10.1021/acscatal.8b02844.
17. W. Xu, Q. Zhang, Q. Shao, C. Xia, M. Wu,Photocatalytic C−F Bond Activation of Fluoroarenes, gem - Difluoroalkenes and Trifluoromethylarenes. Asian Journal of Organic Chemistry. 10, (2021), 2454-2471, https://doi.org/10.1002/ajoc.202100426
18. Q. Guo, Y.Zhang, J. Qiu, G. Dong, Engineering the electronic structure and optical properties of g-C3N4 by non-metal ion doping. Journal of Materials Chemistry C, 4, (2016), 6839–6847, DOI https://doi.org/10.1039/C6TC01831A.
19. Y. Yuan, L. Zhang, J. Xing, M. I. B. Utama, X. Lu, K. Du, … Q. Xiong, High-yield synthesis and optical properties of g-C3N4. Nanoscale, 7,(2015), 12343–12350, DOIhttps://doi.org/10.1039/C5NR02905H
20. Y.Zhang, S. Zong, C. Cheng, J. Shi, P. Guo, X.Guan, … L.Guo, Rapid high-temperature treatment on graphitic carbon nitride for excellent photocatalytic H 2 -evolution performance. Applied Catalysis B: Environmental, 233, (2018)80–87. doi: 10.1016/j.apcatb.2018.03.104
21. J. Zhang, L. Dai, Heteroatom-Doped Graphitic Carbon Catalysts for Efficient Electrocatalysis of Oxygen Reduction Reaction. ACS Catalysis, 5, (2015), 7244–7253, https://doi.org/10.1021/acscatal.5b01563
22. M. Yourdkhani, F. Nemati, Y. Rangraz, A. Elhampour, Magnetic selenium-doped graphitic carbon nitride nanocomposite as an effective catalyst support for stabilization of Cu NPs. Diamond and Related Materials, 110, (2020) 108136, https://doi.org/10.1016/j.diamond.2020.108136
23. Z. Li, G. Gu, S. Hu, X. Zou, G. Wu, Promotion of activation ability of N vacancies to N2 molecules on sulfur-doped graphitic carbon nitride with outstanding photocatalytic nitrogen fixation ability. Chinese Journal of Catalysis, 40, (2019), 1178–1186, https://doi.org/10.1016/S1872-2067(19)63364-4
24. Y. Feng, M. Xu, P.-L. Tremblay, T. Zhang, The one-pot synthesis of a ZnSe/ZnS photocatalyst for H2 evolution and microbial bioproduction. International Journal of Hydrogen Energy, 46, (2021), 21901–21911, https://doi.org/10.1016/j.ijhydene.2021.04.024
25. S. Yu, X.-B. Fan, X. Wang, J. Li, Q. Zhang,A. Xia, …G. R. Patzke,. Efficient photocatalytic hydrogen evolution with ligand engineered all-inorganic InP and InP/ZnS colloidal quantum dots. Nature Communications, 9, (2018), DOI: 10.1038/s41467-018-06294-y.

26. S. P. Lonkar, V. V. Pillai, S. M. Alhassan, Facile and scalable production of heterostructured ZnS-ZnO/Graphene nano-photocatalysts for environmental remediation. Scientific Reports, 8, (2018), DOI:10.1038/s41598-018-31539-7.
27. X. Hong, X. Wang, Y. Li, J. Fu, B.Liang, Progress in Graphene/Metal Oxide Composite Photocatalysts for Degradation of Organic Pollutants. Catalysts, 10, (2020), 921, https://doi.org/10.3390/catal10080921.
28. S.K. Gupta, A. K. Gupta, R. K. Yadav, A. Singh, B. C. Yadav, highly efficient in-situ sulfur doped graphitic carbon nitride nanoplates as an artificial photosynthetic system for NADH regeneration, Vietnam J. Chem., 59, (2021), 590-598, https://doi.org/10.1002/vjch.202000220
29. S. Chaubey, C. Singh, P. Singh, A. Kumar, P. P. Pande, J.-O. Baeg, … R. K. Yadav, Efficient photocatalytic synthesis of l-glutamate using a self-assembled carbon nitride/sulfur/porphyrin catalyst. Environmental Chemistry Letters, 18, (2020), 1389–1395, https://doi.org/10.1007/s10311-020-01004-x.
30. S. Singh, R. K. YadavT. W. Kim, C. Singh, P. Singh, A. P. Singh, A. K. Singh, A. K. Singh, J.-O. Baeg,Rational design of a graphitic carbon nitride catalytic–biocatalytic system as a photocatalytic platform for solar fine chemical production from CO2,React. Chem. Eng., 2022,7, 1566-1572, DOIhttps://doi.org/10.1039/D2RE00079B
31. J. He, C. Janáky, Recent Advances in Solar-driven Carbon Dioxide Conversion: Expectations vs. Reality. ACS Energy Letters.ACS Energy Lett., 5, (2020), 1996–2014, https://doi.org/10.1021/acsenergylett.0c00645
32. R. You, H.Dou, L. Chen, S. Zheng, Y.Zhang Graphitic Carbon Nitride with S And O Codoping for Enhanced Visible Light Photocatalytic Performance, RSC Adv., 7, (2017), 15842-15850, DOIhttps://doi.org/10.1039/C7RA01036B
33. S. Chaubey,R. K., Yadav T. W. Kim, T. C. Yadav,A. Kumar, D.K., Dwivedi,B. K. Pandey, A.P. Singh Fabrication of Graphitic Carbon Nitride-Based Film: An Emerged Highly Efficient Catalyst for Direct C-H Arylation under Solar Light, Chinese J. Chem., 39, (2020),633-639, https://doi.org/10.1002/cjoc.202000470.
34. Y. Li, Z. Jin, L.Zhang, K. Fan Controllable Design of Zn-Ni-P on g-C3N4 for Efficient Photocatalytic Hydrogen Production, Chinese J. Catal., 40, (2019), 390-402, https://doi.org/10.1016/S1872-2067(18)63173-0
35. P. Singh, R. K. Yadav, K. Kumar, Y. Lee, A. K. Gupta, K. Kumar, … T. W. Kim, Eosin-Y and SulfurCodoped g-C3N4 Composite for Photocatalytic Applications: Regeneration of NADH/NADPH and Oxidation of Sulfide to Sulfoxide. Catalysis Science & Technology., Catal. Sci. Technol., 11, (2021), 6401-6410, https://doi.org/10.1039/D1CY00991E
36. G. Liu, X. Qiao, M. A. Gondal, Y. Liu, K.Shen, Q. Xu,. Comparative Study of Pure g-C3N4 and Sulfur-Doped g-C3N4 Catalyst Performance in Photo-Degradation of Persistent Pollutant Under Visible Light. Journal of Nanoscience and Nanotechnology, 18, (2018),4142–4154, https://doi.org/10.1166/jnn.2018.15243.
37. M. Kaur, K. Pal, Synthesis, characterization and electrochemical evaluation of hydrogen storage capacity of graphitic carbon nitride and its nanocomposites in an alkaline environment. Journal of Materials Science: Materials in Electronics, 32, (2021), 12475–12489, 10.1007/s10854-021-05882-x
38. N. Matthias, F Stefan, B König, K Zeitler, Metal-Free, Cooperative Asymmetric Organophotoredox Catalysis with Visible Light. Angew. Chem. Int. Ed. 50, (2011), 951 –954, https://doi.org/10.1002/anie.201002992
39. C. L. Pitman, O. N. L. Finster, A. J. M. Miller, Cyclopentadiene-Mediated Hydride Transfer from Rhodium Complexes. Chem. Commun. 52,(2016), 9105–9108, DOIhttps://doi.org/10.1039/C6CC00575F
40. K. Burton, T. H. Wilson, The Free-Energy Changes for the Reduction of Diphosphopyridine Nucleotide and the Dehydrogenation of L-Malate and L-Glycerol 1-Phosphate. Biochem. J. 54, (1953), 86-94, doi: 10.1042/bj0540086
41. Y. Wu, J. Ward-Bond, D. Li, S.Zhang, J.Shi, Z.Jiang, g-C3N4@α-Fe2O3/C Photocatalysts: Synergistically Intensified Charge Generation and Charge Transfer for NADH Regeneration. ACS Catalysis, 8, (2018), 5664–5674, https://doi.org/10.1021/acscatal.8b00070
42. S. K. Choi, H. S. Yang, J. H. Kim, H. Park, Organic Dye-Sensitized TiO2 as a Versatile Photocatalyst for Solar Hydrogen and Environmental Remediation. Appl. Catal. B Environ. 121, (2012), 206-213, https://doi.org/10.1016/j.apcatb.2012.04.011
43. F. Hollmann, B. Witholt, A. Schmid, [Cp∗Rh(bpy)(H2O)]2+: A Versatile Tool for Efficient and Non-Enzymatic Regeneration of Nicotinamide and Flavin Coenzymes. J. Mole. Catal. B Enzym., 19, (2002), 167-176, https://doi.org/10.1016/S1381-1177(02)00164-9

44. R. K. Yadav, J.-O. Baeg, G. H. Oh, N.-J. Park, K. Kong, J. Kim, … S. Biswas, K. A Photocatalyst–Enzyme Coupled Artificial Photosynthesis System for Solar Energy in Production of Formic Acid from CO2. Journal of the American Chemical Society, 134, (2012), 11455–11461, https://doi.org/10.1021/ja3009902
45. R. K. Yadav, G. H. Oh, N.-J. Park, A. Kumar, K. Kong, J.-O. Baeg, Highly Selective Solar-Driven Methanol from CO2 by a Photocatalyst/Biocatalyst Integrated System. Journal of the American Chemical Society, 136, (2014), 16728–16731, https://doi.org/10.1021/ja509650r.
46. R. K. Yadav, A. Kumar, D. Yadav, N.-J. Park, J. Y. Kim, J.-O. Baeg, In Situ Prepared Flexible 3D Polymer Film Photocatalyst for Highly Selective Solar Fuel Production from CO_2. ChemCatChem, 10, (2018). 2024–2029, https://doi.org/10.1002/cctc.201701730
47. L. E. Oi, M.-Y. Choo, H. V. Lee, H. C. Hamid Ong, S. B. A.,J. C. Juan, Recent advances of titanium dioxide (TiO2) for green organic synthesis. RSC Adv., 6, (2016), 108741−108754, DOIhttps://doi.org/10.1039/C6RA22894A
48. H. Cheng, W. Xu, Recent advances on modified-TiO2 in photo-induced organic synthesis. Org. Biomol. Chem. 17, (2019), 9977–9989.DOI https://doi.org/10.1039/C9OB01739A.
49. L. Ravichandran, K. Selvam, M. Muruganandham, M. Swaminathan, Photocatalytic cleavage of C–F bond in pentafluorobenzoic acid with titanium dioxide- P25. Journal of Fluorine Chemistry, 127, (2006), 1204–1210, https://doi.org/10.1016/j.jfluchem.2006.06.009
50. L. Hong, X.Penglogo, L.Nie, L. Zhou, M. Yang, F. Li, J. Hub, Z. Yao Liangxian Liu, Graphene oxide-catalyzed trifluoromethylation of alkynes with quinoxalinones and Langlois' reagent, RSC Adv., 11, (2021), 38667-38673, https://doi.org/10.1039/D1RA07014B